

Curvature Profiles as Starting Conditions for the Creation of Primordial Black Holes

Dr. Durgesh Wadhwa¹, and Dr. Gopal Arora²

^{1,2}Assistant Professor, Department of Chemistry, Sanskriti University, Mathura, Uttar Pradesh, India

Correspondence should be addressed to Dr. Durgesh Wadhwa; hodchem@sanskriti.edu.in

Copyright © 2022 Made Dr. Durgesh Wadhwa et al. This is an open-access article distributed under the Creative Commons Attribution License, which permits unrestricted use, distribution, and reproduction in any medium, provided the original work is properly cited.

ABSTRACT- This research is part of a larger project to look at the development there were a number of primordial black holes during the radiation-dominated phase of the early universe (PBHs). We offer a beginning arrangement in dimensions of a curving profile, which encapsulates initial circumstances for higher intensity metric disruptions while staying away first from undifferentiated Newman framework, which again is essential for PBH formation, while operating within hexagonal symmetry. When the variance of both the structure is significantly bigger than the cosmic boundary, we employ an iterative bordering answer to connect the bends curve to the spectrometric work and motion fields, which may have been considered of as minor perturbations of the average results at an acceptable enough period. For volume and velocity profiles, we propose broad analytic solutions. These discoveries allow us to look into the personality creation of PBHs in a range of cosmological settings, where the cosmic fluid can be seen as an infinite mix of numerous components of complex equations of state. As a result of the start time, we give analytical answers for volume and mobility characteristics. After that, two different approaches are used to define the curved.

KEYWORDS- Black Hole, Curvature, Primordial, Generic, Velocity.

I. INTRODUCTION

Zeldovich and Novikov suggested the in 1966, Einstein hypothesized the Hawking suggested the possibility of primordial black holes (PBHs), while them in the early 1970s. It was subsequently hotly contested in the following decades (for a detailed list of sources, see, for examples, Carr's latest review). Feynman was a genius. The renowned finding of black hole evaporation in 1974, which is cosmologically significant if the black hole mass is less than 1015 g. As a result, the issue of PBH creation became more appealing, and it was extensively researched during the next 30 years. Carr (1975) used a simple To examine the PBH generation process, researchers created a spherical Provides indexing (Approximately usd) galaxy with a physically flat Http expanding backdrop is used to represent an excessively dense collapsing area. Thus resulting in a thorium age of the planet's thorium epoch of world's radon century of both the world's predefined threshold for said perturbations height c , where the significance is given

also as material overflow in the over dense region and the black holes generated contain dimensions on the range of the frontier size at the time of formation. Moore was able to infer a previous guess of $c \approx 1/3$ by contrasting the Judges wavelength with both the cosmic threshold scale now at age of black hole formation [1]–[4].

Following [5] that, in 1978 [6] and 1980 Andizhan, Novikov, and Polnarev performed an inner hydro kinetic study of PBH creation utilizing, during the first instance in this application, a freshwater kinetic computer code implemented in the Blacksmith language, distinguished by an orthogonal measurement with a geological time coordinates that, as in event of aberrations, simplifies to that same FRW metric. Pouters and May and White have previously employed the similar slicing to investigate stellar core collapse. Bicknell and Hendrickson [produced an alternate study in 1979 a new method relies on synthesis of viscous dissipation characteristics the maximum intensity of the displacement was proven in any of these experiments. is influenced by the geometry of the starting circumstances. Pressure gradients were also discovered in [6] to significantly decrease the Somewhere at end of the multiphase flow operation, PBH material is created [7].

[8]over the next 20 years, researchers focused on several elements of PBH development. Measuring fair value of Deleterious energy released by tiny PBHs with sizes fewer about 1200 g, for example, can set significant limitations on factors essential dictate the planet's many periods of evolution. events . Phase transformations, a nonlinear equation of state cosmological loop closure, and bubbly interactions have all been investigated as potential sources of PBH. PBH research study provides a different investigation for a wide range of fundamental subjects, including early universe, cosmological models, collapsing collapse, even increased thermodynamics. This would be detailed in the many PBH assessments, which provide extensive identified articles [3].

Niemeyer and Jedamzik reported new numerical calculations in 1999 that demonstrated the significance of trying to scale laws in the evolution of PBHs. They showed that if is close enough though to c , that black matter mass Providers must be able follows a hooke's law (c), similar to what Choptuik and others observed in critical collapse. $C \approx 0.7$ was found for all Niemeyer and Jedamzik looked at three different kinds of perturbations models. Due to a mixture and Sasaki proposed a new methodology for analyzing PBH formation just last year, concentrating on measuring perturbations but instead of

percentage interruptions, as was done before. They pointed out that the starting circumstances in were generated within a multifunctional region of oscillations in the thermodynamic efficiency and acceleration area, and were always polluted by an irreversible faded mode fraction that may deviate at $t = 0$. This was recently published in a report. technique was transformed in parameters of perturbations strength, showing that the Due to a mixture and Sasaki results, although correspond to a vast scope of fluctuation types, are consistent with c in the spectrum $0.3 < c < 0.5$ [9]–[12].

Musco discussed the difference here between $c = 0.7$ by training a model equivalent to these other in but describing the boundary values in within system. A typical of power output disruptions, resulting in only rapidly increasing Bending profiles as system parameters for primordial black top to bottom now at heavenly hemisphere passing time, approaches 1407 alternatives. For that very same sorts of disruptions patterns employed in, simulations in give values of ca as in order of 0.43–0.47. The current situation research is a first-of-its-kind exploration of PBH creation that uses the normal approximation introduced in, but also a sort of pseudo resolution that may be characterized by a singular radial reference functional assuming round asymmetry. Throughout this article, this function, designated by $K(r)$, is used as a bender factor to allow for inner computation soundness throughout the whole set the starting conditions. Nadezhin, Novikov, plus Polnarev's initial methodology has been developed further.

According with exponential equivalent to an increasing lateral perturbations of the measurement does not depend on time, but fluctuations of power output as well as velocities vanish convergence rate as $t \rightarrow 0$. As a consequence, they may be classified as mild annoyances. By numerical solution for minuscule velocity and population shocks analytical, researchers force all of the beginning team dynamics to a moment in time where the borderline solution of a proper pattern is feasible in an identity way. The curves profile $K(r)$ stands as the generator on the top right of the appropriate formulations, and we may say that such gravimetric energy and velocities changes that. To avoid any confusion, it's vital to highlight that any cosmological model's minor perturbations are only meaningful in this respect by computing the likelihood of finding a combination with a big volume meter distortion. In reality, the tiny density and velocity perturbations we describe here are completely controlled by the curvature profile inside the starting configuration, rather than being linear cosmic beginning conditions[13].

The following is a breakdown of the paper's structure. We provide a very short explanation Section 2 contains the Misner–Sharp equations. These equations are then used to represent all of the initial conditions. For example of something like a curving characteristics, that we can After that, we'll employ it in our calculations. Once the fluctuation of any of the configuration is substantially larger than the astronomy vista, the Misner–Sharp formulae may indeed be simplified to a single term. Set containing regular differentiated numerical integration empirically. We develop solutions for every mix of ideal gases, which would be a very common scenario. We reveal that commensurate disruptions of power output

and kinetic energy achieved inside this guideline of the proto workaround grow both with time especially like the a genuine expanding phase in conventional astrophysical calculations, while his/her air economy depends is entirely decided by the contour profile K , there in simple consists of a sole channel flow (r) [14]–[16].

The physical characteristics in segment 4, the deformation profile K is explored (r) . In section 5, we provide two different estimation methods of K . (r) . We give information from data. Experiments in section 6 to show that the starting conditions are self-consistent. Moreover, in the event of a plutonium population, we show that the borderline system provides beginning assumptions have been systematically applied in the code but also exhibit numerical examples of primitive black hole formation. We demonstrate how the curvature profile is related to the black hole generation threshold and analyze the findings obtained using the two distinct parameterizations' utilized in the calculations. The rightmost figure in Figure 1 depicts the curves characteristic $K(r)$ as a proportion of something like the commoving vectors for three distinct constants of $(0, 0.5$ and $1)$. This same related contours of the power output perturbations e are presented as parameters of Z in the totally correct figure. These examples, as well as those in the following illustration, were estimated using $\alpha = 1/3$ (equal to $\alpha = 2/3$).

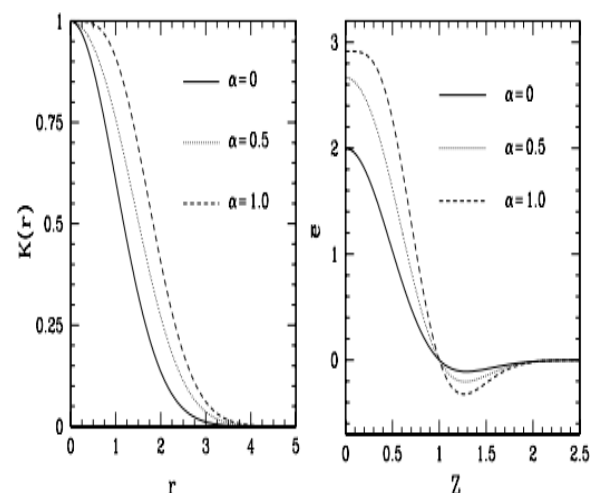


Figure 1: displays the curves gradient $K(r)$ as a proportion of something like the commoving vectors for three separate values of the parameter inside this rear figure $(0, 0.5$ and $1)$. The related patterns of the power output perturbations e are presented as factors of Z in the right-hand figure. These examples, many of which are in the following figures, were estimated using $\alpha = 1/3$ (equal to $\alpha = 2/3$) [17].

II. DISCUSSION

reaction may be shown to be very limited[25]. The hydrodynamical characteristics of black hole creation calculated using starting circumstances given are identical in terms of a bending profile to results reported in, which used the same numerical approach. When observer time slicing was utilized, two sample cases corresponded while galactic clusters slicing was applied, two selected

instances correlated to no black hole growth, whereas 1424 A G Polnarev and I Musco black whole formations. The version is distinguished by a unique value for things like intensity disruptive severity, but it is important to keep track of these values. Incorporate a measure that is different under different scale can use when establishing the beginning conditions at this stage. We see from equations that if we define N_2 in the scenario of constant, the statement transforms time independent, producing in the radiating epoch = $2.3K(r_0)r_2$.

When we compare this number to the value at the horizon crossing, we see that they are on the same scale. As a consequence, we'll refer to as the frequency of population disruptions for the rest of the discussion. The limit intensity c distinguishes amongst stimuli those that disintegrate into black holes, but those that scatter into noise this number was calculated mathematically by performing a converging series of arithmetic operations until gain value was precisely specified. is the metric. When utilizing outsider slicing, a black block is drilled when both slipped f and $+U$ trend near zero. This requirements are convergence rate obtained and are connected to the creation of a ring around an artificial boundary either with an infinite breadth or a finite width as viewed from afar. The recorded moment u is reduced to correspond to timely basis as seen by a regular FRW fundamental observers at the same location. Beyond the perturbations impact spectrum at the grid's outer edge. To achieve this scaling, the outer edge of the grid is set to $f = 1$.

To demonstrate the two cases of black hole generation, we draw at the starting time, a midway period, and a final time, indicated as u_0 , u_i , and u_f , graphs of the radically different Velocity, slip f , the setpoint proportion, and therefore the mass M as factors of the circumference radius Rare shown. For two distinct levels of (c) , black holes develop, with the negative sign culminating together in black orifice with either a lighter weight. The movement of something like the rated velocity U is seen in the upper middle plots of all these two pictures. Start from the top of the curve, the time sequence proceeds downward. It's worth noting that after a given amount of time, U turns minus there in create a place, and the visual threshold (where $2M/R = 1$) disappears. Emerges at the radial velocity profiles lowest. A negative velocity intermediate shell outside of this area corresponds to stuff emitted photons into the black hole, followed by a higher frequency zone corresponding to the rest of the expanding cosmos.

The top right-hand graphs show overall action of the lapses parameter f with the dataset of curves provided by f 's decreasing central value. It can be seen that in the central area, where a black hole is developing, a plateau arises and the lapse gets smaller arithmetically. As said before, one of the main prerequisites for black hole development is the 'halt' the progress. The entrapped perimeter demand ($+U = 0$), roughly equates to $2M/R = 1$, is just another crucial aspect of black hole formation. The development of 1425 primeval black holes began with the use of bending maps as a preliminary step. A typical sequence of events ultimately leads to the development of a black hole is as follows: The beginning curving profile is influenced by the strength of 0 and 1.02, yielding $(c) = 1.3 \cdot 10^2$ degrees. The top plots depict both adaptive optics

U/c and lapses f with mode, while an bottom plots depict $2M/R$ and μ profiles. u_0 , u_p , but of designate the beginning, midway, and ultimate times, respectively., respectively [18].

$2M/R$ is shown arithmetically decrease to 1 at the zenith of the graph as in bottom left graphs. The way the perceived horizon seems to develop is dictated by this. The decreasing $2M/R$ values inside this plot's bottom right demonstrate the causal relationship of the shapes in this example, followed by the climbing of the minimal of all these shapes near 1. Finally, the graphs in the lower right corner. Demonstrate how the mass M , which represents the energy of the black hole formed, behaves. Some curves beginning to converge late in the game. Figures 7 and 8 have had their circumference radius R as well as mass M normalized to the value for the astronomical barrier. With $c = 4.46 \cdot 10^3$ and $(c) = 0.45$, the left-hand figure displays a tiny curvature disturbance far from the threshold c . Because the core area increases more swiftly than with the source image at beginning, negative speed are never obtained. After 1426, [8] [19]–[24].

Figure number eight. The starting curving profile is determined by $= 0.8$ and $= 0.18$, yielding in $(c) = 1.8 \cdot 10^3$, which is an example of a standard scenario that leads to the formation of a black hole The shapes showing dipole scattering U/c plus delay f with time are shown in the central figures, while an courses of $2M/R$ and mass M are shown in the bottom panels. u_0 , u_i , and of designate the beginning, median, and terminating times, respectively. Once the skyline is in sight crossed, the perturbations is dampened, and a compressing wave foments outwardly via the expanded material. In the right-hand picture, the other occurrence is for $(c) = 2.67 \cdot 10^2$. In this case, the disruption frequency of 0.49 is nearly enough as to $c = 1.33$ to cause the core area to collapse prematurely. The crushing material rebounded, creating a compressed wave and stretching further since this strong force was not intense enough yet to form deserted areas. Its continuum mechanics characteristics were initially discovered in [6], but they were subsequently researched in. The calculations have resulted in a component limits appropriate to black hole production for the bending curves described became discovered (105). Figure 10 shows a summary of the results. Given results obtained at various quantities of and used in conceptualization (94), even with field separated into three discrete zones. No black hole creation, black hole development, and unconnected configurations ($K(r)r^2 = 1$). The area of parameters related to black-hole c

III. CONCLUSION

We imposed starting conditions for PBH creation using the quasi-homogeneous solution by adding K is a curvature profile that is independent of time (r). The only source of fluid number interruptions would this be profile, and indeed the disruptions function as clear expansion ways. In the fairly broad circumstance where matter may very well be considered as either an indefinite blend of ideal fluids, we have achieved a mathematical formulation to the Misner–Sharp frameworks of equation defining start changes of concentration variation movements in relation of the bends contour $K. (r)$. For

this, we used computational techniques. $\tau = 1/3$ for two different parameterizations of K to ensure that these beginning conditions were self-consistent (τ). Using a bending profiling to offer beginning circumstance seems to have been advantageous in the analysis of such PBH creation event since it permits for identity system parameters for any and all relevant viscous dissipation components. We recently demonstrated that for steeper K profiles, the generation of PBHs demands higher amplitude and phase of serious meter deviation (τ). As a consequence, generation. In this case, we observed $c = 0.45$, which is consistent with. The results of the two different curvature profile parameterizations demonstrated that the form of the starting profile is crucial for the growth of PBH. This is one of the main reasons for assessing the chance of having different curvature profiles (continuing process) and comparing it to PBH statistics. Potential cosmology models are constrained by observed upper range on PBHs. should be substantially improved as a result of such a connection.

REFERENCE

- [1] S. Leutheusser and M. Van Raamsdonk, "Tensor network models of unitary black hole evaporation," *J. High Energy Phys.*, 2017.
- [2] U. Sharma and I. M. Sheikh, "Investigating self-compacting-concrete reinforced with steel & coir fiber," in *Materials Today: Proceedings*, 2021.
- [3] I. A. Wani and R. ul Rehman Kumar, "Experimental investigation on using sheep wool as fiber reinforcement in concrete giving increment in overall strength," in *Materials Today: Proceedings*, 2021.
- [4] D. Pathak, R. Pratap Singh, S. Gaur, and V. Balu, "To study the influence of process parameters on weld bead geometry in shielded metal arc welding," in *Materials Today: Proceedings*, 2021.
- [5] B. P. Abbott et al., "The basic physics of the binary black hole merger GW150914," *Ann. Phys.*, 2017.
- [6] F. Belgiorno and M. Martellini, "Black holes and the third law of thermodynamics," *Int. J. Mod. Phys. D*, 2004.
- [7] G. T. Horowitz, J. E. Santos, and C. Toldo, "Deforming black holes in AdS," *J. High Energy Phys.*, 2018.
- [8] H. Stöcker, B. Koch, and M. Bleicher, "An introduction to mini black holes at LHC," in *Brazilian Journal of Physics*, 2007.
- [9] J. M. M. Senovilla, "Black holes and trapped surfaces," in *AIP Conference Proceedings*, 2010.
- [10] S. Stojković, S. Oklevski, O. P. Jasuja, and M. Najdoski, "Visualization of latent fingerprints on thermal paper: A new method based on nitrogen dioxide treatment," *Forensic Chem.*, 2020.
- [11] A. Agarwal, "Neuralgic Amyotrophy of Posterior Interosseous Nerve: A Cryptic and Crucial Entity," *Journal of Ultrasound in Medicine*. 2021.
- [12] J. Rai, R. C. Tripathi, and N. Gulati, "A comparative study of implementing innovation in education sector due to COVID-19," in *Proceedings of the 2020 9th International Conference on System Modeling and Advancement in Research Trends, SMART 2020*, 2020.
- [13] C. Stornaiolo, "Cosmological black holes," *Gen. Relativ. Gravit.*, 2002.
- [14] A. Agarwal, S. Agarwal, A. Lalwani, R. Najam, and A. Kumar, "Fetal bradyarrhythmia causing hydrops fetalis: A journey from fetal echo to autopsy," *Ultrasound*, 2020.
- [15] S. Goel, A. Malhotra, A. Agarwal, S. Chandak, A. Kumar, and A. Khan, "Comparative Efficacy of Ultrasonography and Acoustic Radiation Force Impulse (ARFI) Elastography in Prediction of Malignancy in Thyroid Nodules," *J. Diagnostic Med. Sonogr.*, 2020.
- [16] A. Agarwal and S. Agarwal, "Fetal micromelia, thoracic dysplasia and polydactyly revisited: A case-based antenatal sonographic approach," *Ultrasound*, 2019.
- [17] A. Agarwal, S. Agarwal, and S. Chandak, "Role of acoustic radiation force impulse and shear wave velocity in prediction of preterm birth: a prospective study," *Acta radiol.*, 2018.
- [18] A. Gaurav, M. R. Yadav, R. Giridhar, V. Gautam, and R. Singh, "3D-QSAR studies of 4-quinolone derivatives as high-affinity ligands at the benzodiazepine site of brain GABAA receptors," *Med. Chem. Res.*, 2011.
- [19] A. Sesana, "Black Hole Science With the Laser Interferometer Space Antenna," *Frontiers in Astronomy and Space Sciences*. 2021.
- [20] M. David, J. Nian, and L. A. Pando Zayas, "Gravitational Cardy limit and AdS black hole entropy," *J. High Energy Phys.*, 2020.
- [21] H. Z. Chen, Z. Fisher, J. Hernandez, R. C. Myers, and S. M. Ruan, "Evaporating black holes coupled to a thermal bath," *J. High Energy Phys.*, 2021.
- [22] A. Davey, O. J. C. Dias, and P. Rodgers, "Phase diagram of the charged black hole bomb system," *J. High Energy Phys.*, 2021.
- [23] P. Charalambous, S. Dubovsky, and M. M. Ivanov, "On the vanishing of Love numbers for Kerr black holes," *J. High Energy Phys.*, 2021.
- [24] A. Giveon and N. Itzhaki, "Stringy information and black holes," *J. High Energy Phys.*, 2020.
- [25] S. Hod, "A mystery of black-hole gravitational resonances," *J. Cosmol. Astropart. Phys.*, 2016.